Nuclear Engineering and Technology 55 (2023) 4266–4273

Contents lists available at ScienceDirect

Nuclear Engineering and Technology

journal homepage: www.elsevier.com/locate/net

Original Article

Study of contact melting of plate bundles by molten material in severe reactor accidents

J.J. Ma, W.Z. Chen *, H.G. Xiao

College of Nuclear Science and Technology, Naval University of Engineering, Wuhan, 430033, China

ARTICLE INFO

Keywords:
Contact melting
Core melting
Plate bundles
Severe reactor accident

ABSTRACT

In a severe reactor accident, a crust will form on the surface of the molten material during the core melting process. The crust will have a contact melting with the internal components of the reactor. In this paper, the contact melting process of the molten material on the austenitic stainless steel plate bundles is studied. The contact melting model of parabolic molten material on the plate bundles is proposed, and the rule and main effect factors of the contact melting are analyzed. The results show that the melting velocity is proportional to the slope of the paraboloid, the heat flux and the distance between two plates ***D***. The influence of melt gravity and the plate width on melting velocity is negligible. The thickness of the molten liquid film is proportional to the heat flux and plate width, and it is inversely proportional to the gravity. With the increase of ***D***, the liquid film thickness decreases at first and then increases gradually. The liquid film thickness has a minimum against ***D***. When the width of the plate is small, the width of the plate is the main factor affecting the thickness of the liquid film. The parameters are coupled with each other. In a severe reactor accident, the wider internal components of reactor, which can increase the thickness of the melting liquid film and reduce the net input heat flux from the molten material to the components, are the effective measures to delay the melting process.

1. Introduction

The core melting accident is caused by the temperature rise and melting of the exposed core, which cannot be fully cooled. The core melting is a complex systematic process, and a lot of experimental research has been done internationally to simulate the melting process [1]. In the core melting accident, with the continuous generation of decay heat, some core materials begin to melt and form molten materials. The molten materials are surrounded by high temperature steam or cooling debris in the development process, which will form a crust outside the molten to keep it in its original state. The crust of the high-temperature molten is extruded and melted with the reactor components (such as support plates, fuel elements, etc.) under its own gravity [2]. Generally, the core melting behavior can be effectively evaluated through the system code [3]. However, it is impossible to effectively simulate the melting process of specific reactor internals and conduct the rational research on their melting behavior [4]. In addition, different types of molten pool structures will be formed in the lower plenum of reactor vessel due to different metal fraction in the molten material [5]. The focusing effect of the corium pool metal layer may lead to the failure of the lower head of the pressure vessel, and is closely related to the quality of the molten pool metal layer [6]. In a severe accident, the lower core support structure, barrel and other internal components are the main mass sources of the metal layer. Therefore, it is important to study the melting process and melting mechanism of reactor internals for analyzing the pool fraction and pool formation time. For the research on the melting behavior of the internal components, the current theoretical models are mainly the radiation heat transfer model and the melting and solidification model [7]. These models are all non-contact melting models. However, the melting between the corium pool and reactor internals is a typical contact melting. According to existing research, the contact melting will have a melting rate 1-7 times higher than the non-contact or constrained melting under the same operating conditions [8].

Contact melting refers to the melting phenomenon that occurs when solid phase change materials and heat sources extrude each other and the heat source temperature is higher than the melting temperature of phase change materials [8,9]. It is currently applied to the latent heat thermal storage system, passive cooling, food industry, subtractive machining, etc. [10]. Many scholars, such as Emerman et al. [11],

* Corresponding author.
E-mail address: cwz2@21cn.com (W.Z. Chen).

https://doi.org/10.1016/j.net.2023.08.003
Received 21 October 2022; Received in revised form 22 June 2023; Accepted 2 August 2023
Available online 3 August 2023

Moallemi et al. [12] and Chen et al. [13], have studied the contact melting in the background of nuclear melting, proved its feasibility applying to the nuclear field. At present, there are many contact melting analysis models around heat sources with different geometric shapes, such as flat plates [14,15], cylinders [16], spheres [17,18], elliptical columns [19], etc. The results obtained can well match the experimental results, which also proved the correctness of the theory. In severe accidents, the melting of molten materials on the stainless steel surface belongs to the contact melting of narrow structure phase change materials under the high heat flux. Because the molten reactor internals materials tend to melt multiple stainless steel components at the same time, unlike the continuous single medium model, its melting mechanism is more complex.

It is difficult for molten materials to form the spherical structure used by Emerman et al. [11] under the action of its own gravity. Considering that the parabolic column can better cover other shape characteristics, and according to relevant researches [20,21], the contact melting of parabolic heat source is faster than that of other structures mentioned above, so from the perspective of nuclear safety, we use parabolic column structure to simulate the shape of molten materials. After the reactor shutdown, a large decay heat will be generated. The heat power will drop quickly in a short time, and then tend to decline steadily [22]. The change of decay heat in the melting of components is small and can be ignored, so a constant heat flux is used for the thermal boundary conditions on the surface of the molten materials in modeling and analysis. At the present work, the contact melting analysis model of parabolic column melt on the plate bundles is deduced by reasonable assumptions, and the rules and influencing factors of the melting process are analyzed.

2. Melting mechanism and physical model

2.1. Modeling

Fig. 1a shows the contact melting of molten material of horizontal parabolic column ($y = kx^2$) on two plates, and the plate is parallel to the axis of parabolic column. The width of the parabolic column molten material is $2\boldsymbol{L}$, and the weight is $\boldsymbol{G}$. The plate width $\boldsymbol{d}$ ($\boldsymbol{d \ll L}$) is symmetrically distributed in the center line of the parabolic column. The distance between the two plates is $\boldsymbol{D}$, and their initial temperature is uniform and equals the material melting point temperature $\boldsymbol{T_m}$. Under the action of gravity, the molten material heat source extrudes and heats the lower plate to melt it. In the melting process, a thin but relatively stable liquid film boundary layer is formed between the molten material and the plate. The molten liquid flows out from both sides through the liquid film, and the thickness of the liquid film is recorded as $\boldsymbol{\delta}$. The molten material center moves along the gravity direction, and the velocity is recorded as $\boldsymbol{U}$. Taking the tangent direction of the molten material contact surface as the $\boldsymbol{h}$ axis, and its normal direction as the $\boldsymbol{s}$ axis, the melting coordinates ($\boldsymbol{s}$, $\boldsymbol{h}$) is set up on the molten material surface. The included angle between the normal direction of the melting interface and y-axis is recorded as $\boldsymbol{\theta}$. Since the width of the plate is far less than the that of the molten material, the normal angle of the heat source is approximately equals that of the melting interface [23]. As shown in Fig. 1b, $\boldsymbol{\theta_1}$ is the angle between the normal direction of the melting interface on the side of the plate bundle and the y-axis. $\boldsymbol{\Delta\theta_1}$ is the change of $\boldsymbol{\theta_1}$. Fl in Fig. 1b is the force by pressure in the molten film layer between the plate bundle and heat source.

2.2. Model equations

According to contact melting characteristics and relevant conclusions by Salamatin et al. [24], and Bejan [25], it is assumed as follows.

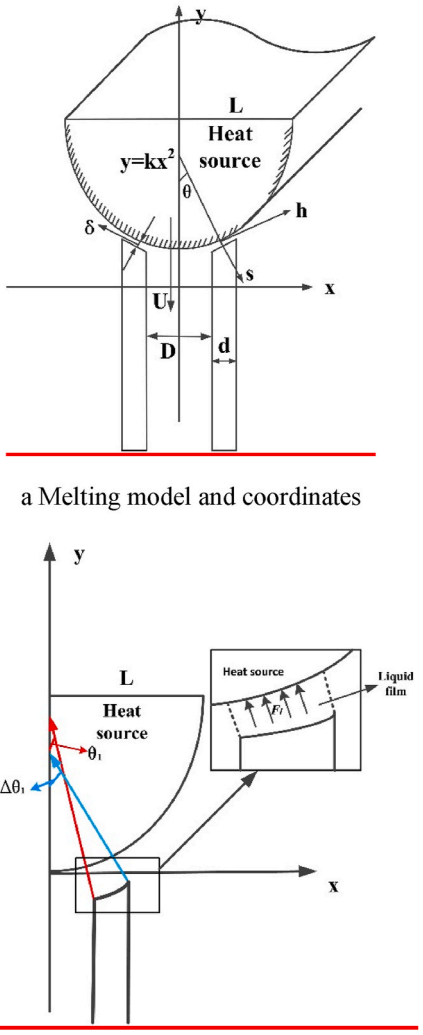

Fig. 1. Physical model and coordinate diagram of double plate melting.

a. The melting velocity is relatively slow, and the melting process can be regarded as a steady uniform movement, which always satisfies the force balance.
b. The liquid pressure in the liquid film does not change in the normal direction ($\boldsymbol{s}$-axis) of the melting contact surface, and the effects of the inertial force, shear stress and convection heat transfer of the fluid are ignored.
c. The thermophysical properties of the plate bundle are isotropic and do not change with temperature.
d. The liquid in the liquid film is Newtonian fluid, and the flow is laminar

According to the assumptions, the conservation equations of fluid energy, momentum and mass in the liquid film are:

$$u\frac{\partial T}{\partial h} + v\frac{\partial T}{\partial s} = a\frac{\partial^2 T}{\partial s^2} \tag{1}$$

$$\mu\frac{\partial^2 u}{\partial s^2} = \frac{dp}{dh} \tag{2}$$

$$\frac{\partial u}{\partial h} + \frac{\partial v}{\partial s} = 0 \tag{3}$$

Because the contact molten liquid film is very thin, the temperature

gradient along the $\boldsymbol{h}$ direction is much smaller than that along the $\boldsymbol{s}$ direction, that is, $\frac{\partial T}{\partial h} \ll \frac{\partial T}{\partial s}$. The heat transfer from the liquid film layer on the outer wall of the parabolic column to the plate can be regarded as one-dimensional heat transfer. Because of $\boldsymbol{d} \ll \boldsymbol{L}$, it can be considered that the s-direction velocity of the fluid in the liquid film can be approximately determined by $\boldsymbol{U}\cos\theta_1$. Then the energy conservation equation can be simplified as:

$$(-\mathrm{U}\cos\theta_1)\frac{\partial T}{\partial s} = \mathrm{a}\frac{\partial^2 T}{\partial s^2} \tag{4}$$

Where a is the thermal diffusivity, $\mathrm{a} = \frac{\lambda}{\rho C_p}$.

The boundary conditions of the liquid film layer are:

$$\mathrm{s} = 0, \frac{\partial \mathrm{T}}{\partial \mathrm{s}} = -\frac{q''}{\lambda}; s = \delta, T = T_m \tag{5}$$

Substituting conditions (5) into Eq. (4) yields to:

$$T(s) = T_m + \frac{\mathrm{a}q''\left[e^{\left(-\frac{Us\cos\theta_1}{\mathrm{a}}\right)} - e^{\left(-\frac{U\delta\cos\theta_1}{\mathrm{a}}\right)}\right]}{\lambda U\cos\theta_1} \tag{6}$$

The melting energy balance equation of the solid-liquid interface is:

$$-\lambda\frac{\mathrm{dT}}{\mathrm{ds}}|_{s=\delta} = \rho_s L_m U\cos\theta_1 \tag{7}$$

Substituting Eq. (6) into Eq. (7) yields to

$$\delta = -\mathrm{a}\frac{\ln\left(\frac{\rho_s L_m U\cos\theta_1}{q''}\right)}{U\cos\theta_1} \tag{8}$$

The boundary conditions of Eq. (2) are:

$$\mathrm{s} = 0, \mathrm{u} = 0; \mathrm{s} = \delta, u = 0 \tag{9}$$

Substituting Eq. (9) into Eq. (2) yields to:

$$\mathrm{u} = -\frac{1}{2\mu}\frac{dp}{dh}(s^2 - \delta s) \tag{10}$$

Substituting Eq. (10) into Eq. (3) and integrating it with respect to s yields to:

$$\frac{\mathrm{d}^2 p}{\mathrm{dh}^2} = \frac{-12\mu U\cos\theta_1}{\delta^3} \tag{11}$$

From the geometric relationship in Fig. 1b, the arc length formula is:

$$\mathrm{dh} = \sqrt{1 + (y')^2}dx \tag{12}$$

Where y' is the slope of the parabolic equation as follows:

$$y' = \tan\theta = 2kx \tag{13}$$

Combining Eqs. (13) and (12), we have:

$$\mathrm{dh} = \mathrm{f}(\theta_1)\mathrm{d}\theta \tag{14}$$

Where $\mathrm{f}(\theta_1)$ is:

$$\mathrm{f}(\theta_1) = \frac{\sqrt{1 + \tan^2\theta_1}}{2\mathrm{k}\cos^2\theta_1} \tag{15}$$

Substituting Eq. (15) into Eq. (11) results in:

$$\frac{d^2 p}{d\theta^2} = f^2(\theta_1)\frac{-12\mu U\cos\theta_1}{\delta^3} \tag{16}$$

According to the boundary conditions, the pressure of the liquid film on the interface at the left and right ends is 0, that is:

$$\theta = \theta_1, p = 0; \theta = \theta_1 + \Delta\theta_1, p = 0 \tag{17}$$

Combining Eqs. (17) and (16) yields to:

$$p = f^2(\theta_1)\frac{6\mu U\cos\theta_1}{{\delta_1}^3}(\theta - \theta_1)(\Delta\theta_1 + \theta_1 - \theta) \tag{18}$$

The force by pressure in the liquid film layer is:

$$F_l = \int_{\theta}^{\theta_1+\Delta\theta_1} p\cos\theta_1 f(\theta_1)d\theta \tag{19}$$

Substituting Eq. (18) into Eq. (19) results in:

$$F_l = \frac{\mu U\cos^2\theta_1 f^3(\theta_1){\Delta\theta_1}^3}{{\delta_1}^3} \tag{20}$$

According to the force balance, the force by pressure in the molten film layer should be equal to the gravity of the heat source:

$$\mathrm{G} = 2F_l = 2\frac{\mu U\cos^2\theta_1 f^3(\theta_1){\Delta\theta_1}^3}{{\delta_1}^3} \tag{21}$$

From the geometric relationship in Fig. 1b, Eqs. (22)–(24) can be written as:

$$\sin\theta = \frac{1}{\sqrt{1 + \frac{1}{4k^2\left(\frac{D}{2}\right)^2}}} \tag{22}$$

$$\cos\theta = \sqrt{1 - sin^2\,\theta} = \sqrt{1 - \frac{1}{1 + \frac{1}{4k^2\left(\frac{D}{2}\right)^2}}} \tag{23}$$

$$\Delta\theta = \arcsin\left(\frac{1}{\sqrt{1 + \frac{1}{4k^2\left(\frac{D}{2}+d\right)^2}}}\right) - \arcsin\left(\frac{1}{\sqrt{1 + \frac{1}{4k^2\left(\frac{D}{2}\right)^2}}}\right) \tag{24}$$

Combining Eqs. 21–24, the melting velocity can be written as

$$\mathrm{U} = \mathrm{f}(\mathrm{k}, \mathrm{D}, \mathrm{d}, \mathrm{q}'', \mathrm{G})$$

The velocity **U** is related to the slope $\boldsymbol{k}$ of the molten material, the distance $\boldsymbol{D}$ between two plates, the plate width $\boldsymbol{d}$, the heat flux $\boldsymbol{q''}$ and the gravity $\boldsymbol{G}$ of the molten material.

3. Results and discussions

According to the melting equations 8 and 21 -(24), the influences of slope $\boldsymbol{k}$, distance $\boldsymbol{D}$ between two plates, plate width $\boldsymbol{d}$ and heat flux $\boldsymbol{q''}$ on the melting are analyzed. The plate material selected here is 1Cr18Ni9Ti stainless steel, and its physical parameters are shown in Table 1 [26]. In order to facilitate the analysis, the AP1000 thermal power is chosen as an example to conduct dimensionless treatment of the heat flux. Where $\boldsymbol{q''_{max}}$ is the full power heat flux of the AP1000.

Fig. 2 shows the change of the melting velocity of the molten material with the heat flux under the conditions of $\boldsymbol{D} = 1$ m, $\boldsymbol{d} = 0.1$ m and $\boldsymbol{G} = 15000$ N, where the slope $\boldsymbol{k}$ of the parabolic column is 0.1, 0.5, 1 and 1.5, respectively. It can be seen from Fig. 2 that the melting velocity increases linearly with the heat flux, which is consistent with the experimental phenomenon by Moallemi and Viskanta [27]. Comparing different slope $\boldsymbol{k}$ curves, the higher the $\boldsymbol{k}$ value is, the greater the slope of the curve of melting velocity versus heat flux is, and the greater the melting velocity is. When the heat flux is lower than 0.5%, the difference

Table 1
The physical parameters of the 1Cr18Ni9Ti type stainless steel.

ρ_f (kg/m^3)	λ_f (W/m·K)	c_{pf} (J/(kg·K)	L_f (J/kg)	μ_f (kg/(m·s))	T_m (K)
7900	26.8	580	2.72×10^5	5.9×10^{-3}	1700

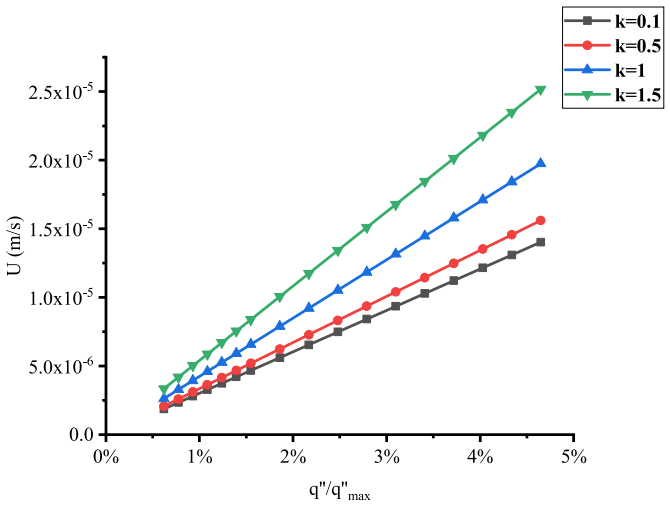

Fig. 2. Changes of melting velocity with heat flux under different slope k.

of melting velocities at different k is small, and they are kept at a low value.

Fig. 3 shows the change of liquid film thickness with heat flux for different slopes of molten paraboloid melted under the conditions of D = 1 m, d = 0.1 m and G = 15000 N. It can be seen from Fig. 3 that the thickness of the liquid film increases monotonously with the heat flux. When the heat flux is small, the slope of the change curve of the liquid film thickness is large, and then decreases with the increase of the heat flux. This shows that the liquid film thickness is more sensitive to the change of heat flux under the condition of low heat flux. Comparing the curves of different paraboloid slopes, it can be found that the greater the slope of the paraboloid is, the greater the thickness of the liquid film is. The heat flux equation is:

$$q'' = \lambda \frac{T_w - T_m}{\delta} \tag{25}$$

Where λ is the thermal conductivity of phase change material, T_w is the surface temperature of the heat source, T_m is the melting point temperature of the phase change material, δ is the liquid film thickness. It can be seen from equation (25) that for the phase change materials whose thermal conductivity does not change with temperature under the same heat flux, the greater the liquid film thickness is, the higher the wall temperature of the heat source required is. It can be seen from Fig. 3 that the higher the heat flux is, the higher the wall temperature required

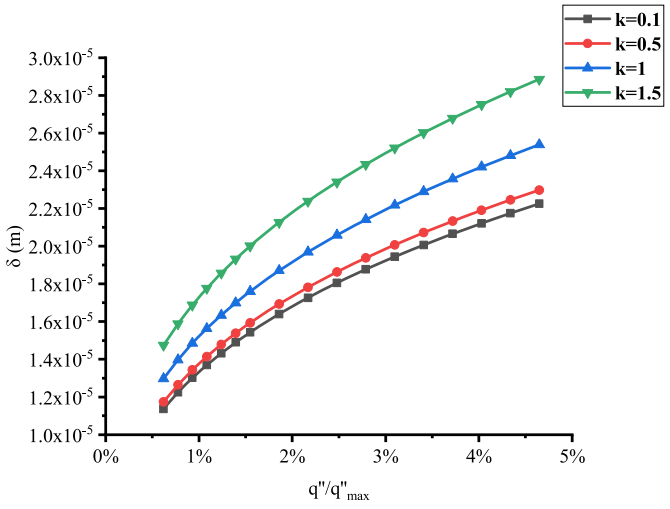

Fig. 3. Changes of liquid film thickness with heat flux under different slope k.

by the surface of the molten material is. Under the same heat flux, the higher the slope k is, the higher the wall temperature required is in the melting process.

Figs. 4 and 5 show the changes of melting velocity and liquid film thickness with the gravity of molten material when k = 1 and D = 1 m, respectively. It can be seen from Fig. 4a that with the increase of the gravity, the melting velocity first increases and then gradually stabilizes. However, when the gravity increases from 5000 N to 30000 N, the change value of melting velocity is within 0.0046%. It can be more clearly seen from Fig. 4b that under the same heat flux, with the increase of gravity, the melting velocity is basically unchanged, which is consistent with the experimental phenomenon by Moallemi and Viskanta [27]. In the actual core melting process, with the melting of the reactor internals, debris keeps falling and accumulating, and the gravity of the melt keeps increasing, but the melting velocity is basically constant. It can be seen from Fig. 4a that the greater the plate width is, the slower the melting velocity is, but the velocity change can be ignored.

It can be seen from Fig. 5 that the thickness of liquid film monotonically decreases with the increase of the gravity of molten material. Fig. 6 is the slope diagram of liquid film thickness changing with gravity. It can be seen from Fig. 6 that when the gravity is small, it has a great influence on the liquid film thickness, and gradually decreases with the increase of gravity. As the gravity of the molten material increases, the liquid film is continuously squeezed, and the force F_l inside the liquid film increases. According to the force balance relationship (22), $\frac{U}{\delta^3}$ is proportional to the gravity G. As shown in Fig. 4, the influence of the gravity G on the melting velocity U is negligible. So δ is proportional to the $\frac{1}{\sqrt[3]{G}}$. It can be also seen from Fig. 5a that the greater the plate width is, the greater the thickness of the liquid film is. This is because the increase of the plate width reduces the pressure on the unit area. By comparing the slope of the change curve of liquid film thickness and gravity under different plate widths and heat flux, as shown in Fig. 6, it can be found that the greater the plate width or heat flux is, the greater the absolute slope of the curve is. This shows that the influence of gravity on liquid film thickness will increase with the increase of plate width or heat flux, especially when the gravity is small.

Fig. 7-10 show the influence of the distance between the plates on melting under the conditions of k = 1 and G = 15000 N. Fig. 7a shows the relationship between the melting velocity and the distance D under different plate width d. It can be seen from Fig. 7a that the melting velocity gradually increases with the increase of plate distances. This is related to the shape of the molten material, and the increase of D indicates the increases of the slope of the contact surface. According to the relationship between the slope and the melting velocity deduced above, the greater the slope is, the faster the melting velocity is, which is consistent with the rule in Fig. 2. In Fig. 7a, the curves of the melting velocity with the plate distance under the different plate width basically coincide, which shows that the influence of the plate width on the melting velocity is very small and can be ignored. Fig. 7b shows the relationship between melting velocity and plate distance under different heat flux. In order to compare the effect of heat flux on D and melting velocity, Fig. 8 shows the slope of melting velocity with D under different heat flux. It can be seen from Fig. 8 that the higher the heat flux is, the greater the slope of the curve of melting velocity changing with D is. Because the melting velocity U is directly proportional to the heat flux q'' with the condition $U = 0$ at $q'' = 0$, as shown in Fig. 2, the melting velocity U can be approximated as $U = Cq''f(D)$, where C is constant. Differentiating the relation with respect to D yields $\frac{dU}{dD} = Cq''\frac{df(D)}{dD}$, so that the value of $\frac{dU}{dD}$ is greater when q'' is higher.

Fig. 9a shows the relationship between the liquid film thickness δ and

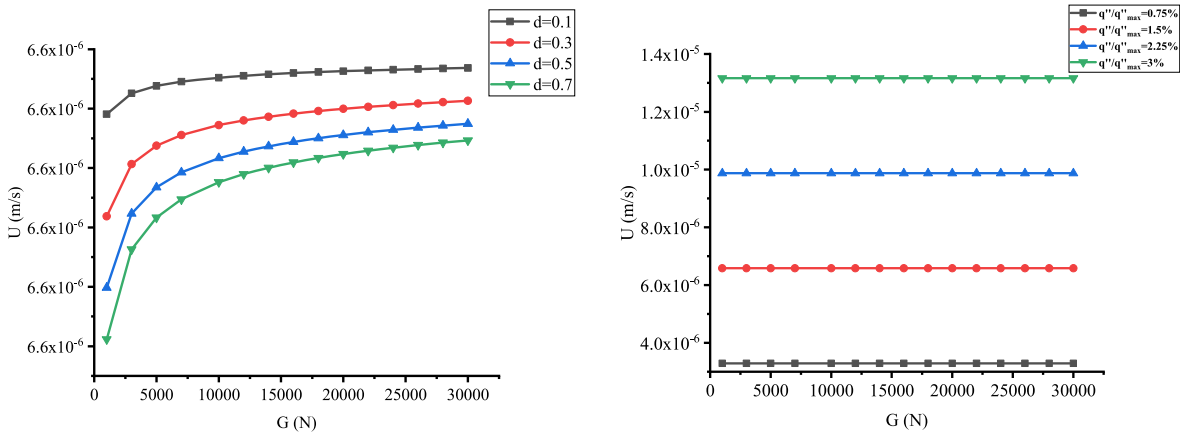

a Under different plate width b Under different heat flux

Fig. 4. Changes of melting velocity with molten material gravity.

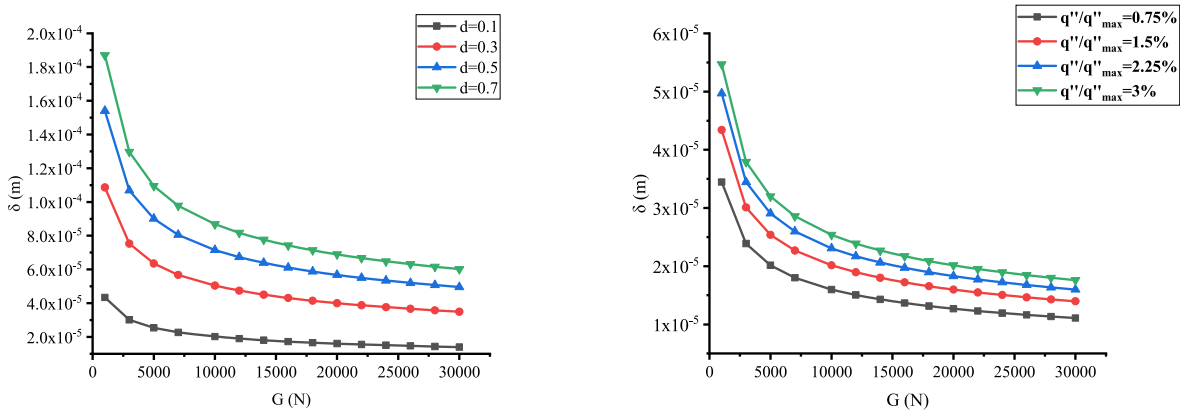

a Under different plate width b Under different heat flux

Fig. 5. Changes of liquid film thickness with molten material gravity.

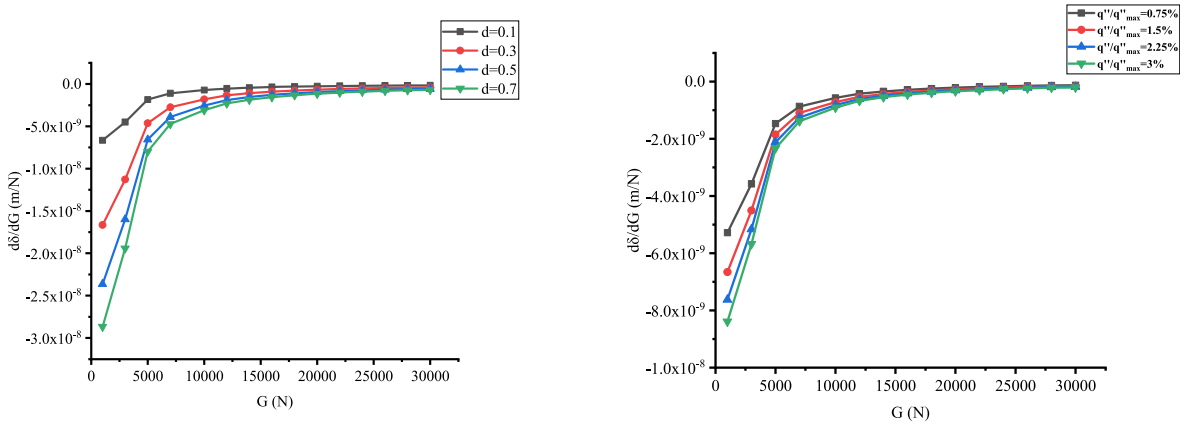

a Under different plate width b Under different heat flux

Fig. 6. Changes of slope of liquid film thickness with gravity.

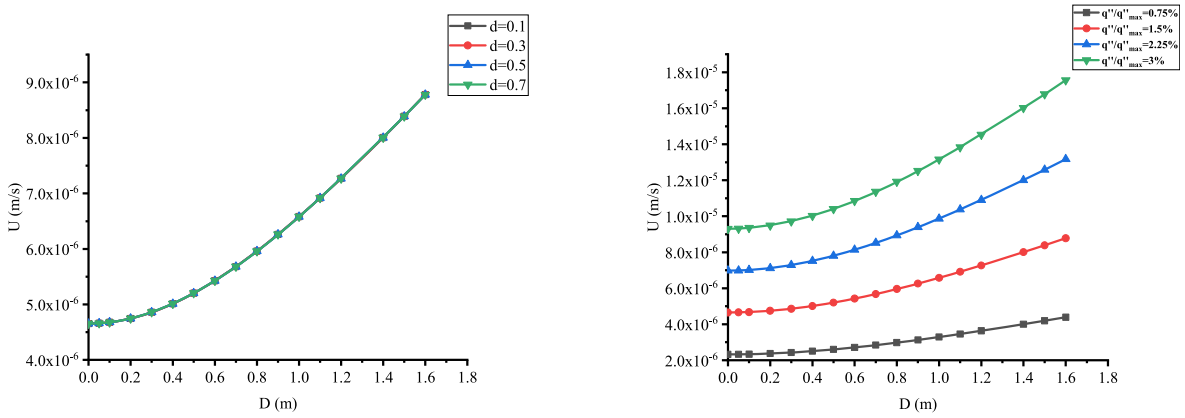

a Under different plate width

b Under different heat flux

Fig. 7. Changes of melting velocity with plate distance.

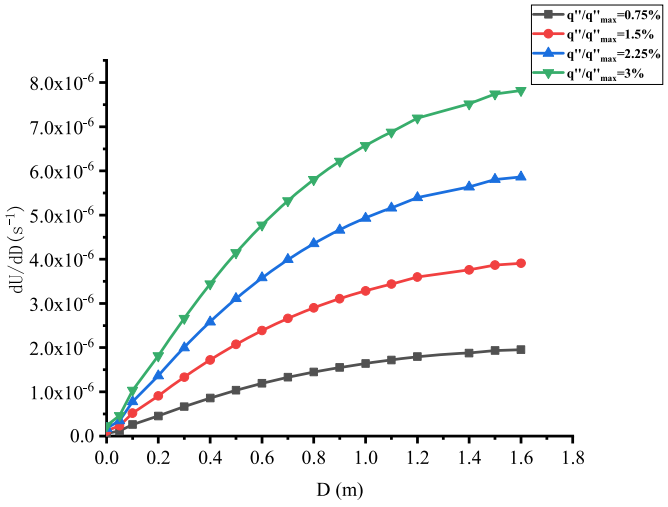

Fig. 8. Changes of slope of melting velocity with plate distance.

the plate distance ***D*** under different plate widths. It can be seen that δ decreases first and then increases gradually with the increase of ***D***. The liquid film thickness has a minimum against ***D***. By comparing the curve slopes under different plate widths, as shown in Fig. 10a, the greater the plate width is, the greater the influence of ***D*** on the liquid film thickness is. When the plate width is small, as shown in Fig. 9a and 10a, ***D*** has little effect on the liquid film thickness and the slope of the curve also remains at a low value for d = 0.1 m, which is consistent with Fig. 5a and 6a. This shows that the plate width is the main factor affecting the liquid film thickness when it is small. According to equation (25), the larger the plate distance is, the higher the melting temperature required on the surface of the molten material is. However, when the plate width is small, the liquid film is always kept at a lower thickness. So the melting temperature required on the surface of the molten material is lower, which is more likely to cause melting. Figs. 9b and 10b show the liquid film thickness changing with ***D*** under different heat flux. It can be found that the higher the heat flux is, the greater the slope of the curve is. This shows that the heat flux will strengthen the effect of ***D*** on the liquid film thickness.

4. Conclusions

Based on the contact melting theory, the analysis model for the molten material to melt plate bundles in severe accidents is obtained. The factors affecting the melting characteristics are analyzed, and the specific conclusions are summarized as follows.

1. The melting velocity and the liquid film thickness are proportional to the heat flux. The thickness of liquid film is sensitive to the change of heat flux under the condition of low heat flux. In the case of high heat

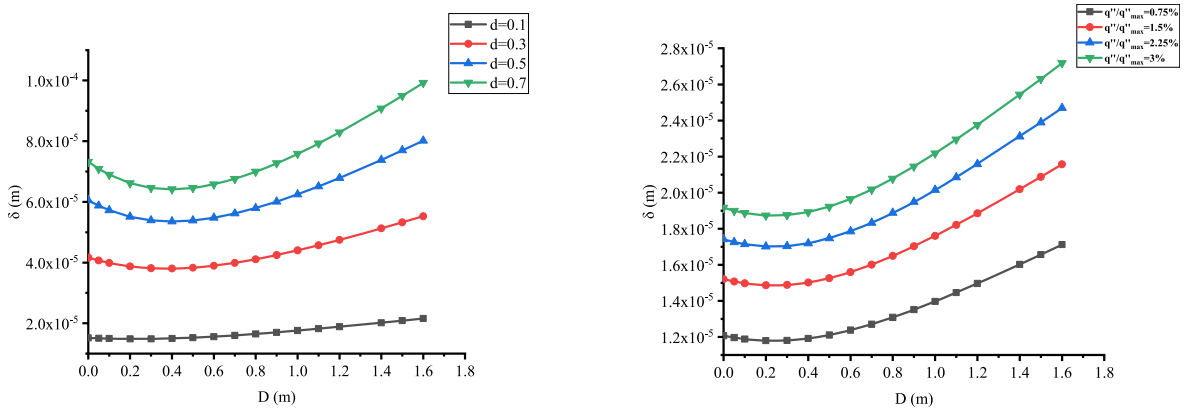

a Under defferent plate width

b Under defferent heat flux

Fig. 9. Changes of liquid film thickness with plate distance.

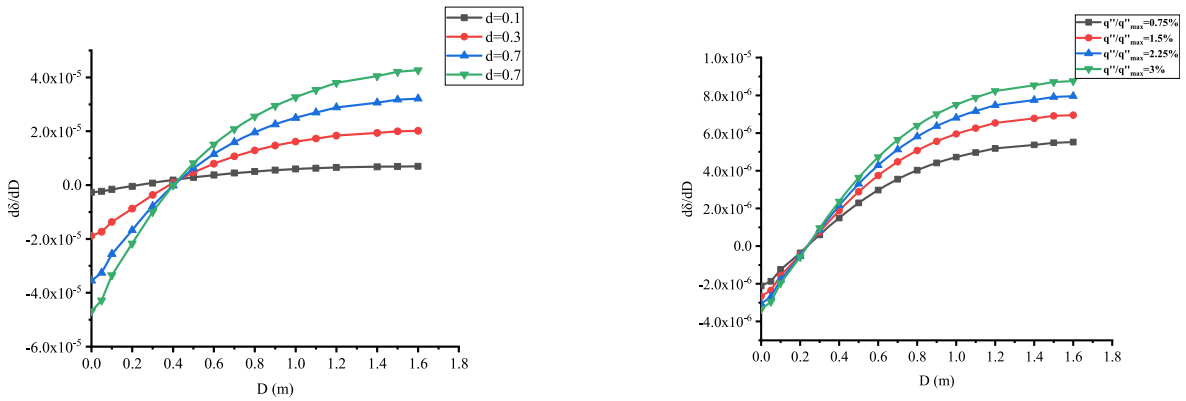

a Under defferent plate width b Under defferent heat flux

Fig. 10. Changes of slope of liquid film thickness with plate distance.

flux, the melting velocity is faster, and the greater the thickness of the liquid film is, the higher the melting temperature required on the surface of the melt is. Therefore, cooling the surface temperature of the molten material under high heat flux can effectively prevent the melting process. For example, in a severe accident, the heat can be removed from the reactor by submerging the core or cooling the pressure vessel walls, thus indirectly cooling the surface temperature of the molten material.

2. The influence of the gravity of molten material on the melting velocity is small and can be ignored. The thickness of the liquid film decreases with the increase of the gravity of the molten material, which is more obvious when the gravity is small. With the increase of the gravity, the change of the liquid film thickness decreases gradually and tends to zero.
3. The influence of the plate width on the melting velocity can be ignored, but it has a great influence on the thickness of the liquid film. The greater the plate width is, the greater the thickness of the liquid film is.
4. The melting velocity increases with the increase of the distance between two plates ***D***. The increasing rate of velocity increases first and then becomes stable with the increase of ***D***; With the increase of ***D***, the liquid film thickness first decreases and then gradually increases, and there is a minimum value of the liquid film thickness against ***D***. When ***D*** reaches a certain value, the melting velocity and liquid film thickness monotonically increase with the increase of ***D***.
5. The high heat flux will strengthen the effect of other parameters on the melting velocity and liquid film thickness. The plate width will strengthen the effect of ***D*** on the liquid film thickness. When the plate width is small, it is the main factor affecting the liquid film thickness. The increase of the slope ***k*** of the molten surface will strengthen the influence of heat flux on the melting velocity, but the melting velocity will remain at a low value when the heat flux is small. The heat flux and plate width will obviously strengthen the effect of gravity on the liquid film thickness when the gravity is small, which will gradually decrease with the increase of gravity.

From the perspective of nuclear safety, in order to ensure the safety of the reactor in severe accidents, we need to reduce the melting velocity and increase the heat transmission resistance, i.e. the larger melt film thickness. According to the above analysis, increasing the plate width of the internal components of reactor is one of the effective way that can be considered for the reactor design to curb melting in a severe accident. Due to the significant impact of the heat flux on melting velocity, during the severe reactor accident, the cavity injection system(CIS) can be used to cool the wall of reactor pressure vessel [28]. Conducting the heat from reactor into cooling fluid of the CIS will indirectly reduce the net input heat flux transmitted by the molten material to the components inside the reactor, thus slowing down the melting process. In addition, considering the influence of gravity of the melting material on the melting, it is necessary to cool the core at the early stage of melting when the debris has not fallen off in large quantities to reduce the surface temperature of the melt. So running the CIS in the early stage of melting has a better effect on the mitigation of the melting process.

Declaration of competing interest

None.

Acknowledgements

This research was financially supported by the National Natural Science Foundation of China (project number 12175311).

References

[1] R.R. Hobbins, D.A. Petti, D.J. Osetek, D.L. Hagrman, Review of experimental results on light water reactor core melt progression, Nucl. Technol. 95 (3) (1991) 287–307.
[2] W.C. Müller, Review of debris bed cooling in the TMI-2 accident, Nucl. Eng. Des. 236 (2006) (2006) 1965–1975.
[3] X. Li, I. Sato, A. Yamaji, Sensitivity analysis of in-vessel accident progression behavior in Fukushima Daiichi nuclear power plant unit 3, Ann. Nucl. Energy 133 (2019) 21–34.
[4] S. Ding, H.F. Huang, R.H. Zhong, X.Y. Zhang, D.K. Zhan, Numerical Analysis of movement and heat transfer of melting material in PWR core, At. Energy Sci. Technol. 1 (2020) (2020) 44 (in Chinese) 54.
[5] F. Fichot, J.M. Bonnet, B. Chaumont, IRSN views and perspectives on in-vessel melt retention strategy for severe accident mitigation, EUROSAFE Forum, Brussels, Nov (2015) 2–3.
[6] Z.H. Guan, Q.A. Xiang, B. Chen, H.X. Yu, Probability analysis for effectiveness of IVR strategy during severe accidents for ACP1000 through ROAAM, Nucl. Power Eng. 6 (2015) 56–60 (in Chinese) 36.
[7] L.Q. Hou, D.H. Zhu, Q. Wu, Y.Z. Liu, Z.D. Liu, H.T. Zheng, Research of behavior of the core shroud and barrel during a severe accident, Nucl. Sci. Eng. 5 (2020) 827–835 (in Chinese) 40.
[8] W.Z. Chen, Analysis of Contact Melting, Chinese Atomic Energy Press, Beijing, 2022 (in Chinese).
[9] V. Cregan, J. Williams, T.G. Myers, Contact melting of a rectangular block with temperature-dependent properties, Int. J. Therm. Sci. 150 (2020), 106218.
[10] H. Nan, Z.R. Li, Z.W. Xu, L.W. Fan, Rapid charging for latent heat thermal energy storage: a state-of-the-art review of close-contact melting, Renewable Sustainable Energy Rev. 155 (2022), 111918.
[11] S.H. Emerman, D.L. Turcotte, Stokes's problem with melting, Int. J. Heat Mass Tran. 26 (11) (1983) 1625–1630.
[12] M.K. Moallemi, R. Viskanta, Analysis of melting around a moving heat source, Int. J. Heat Mass Tran. 29 (8) (1986) 1271–1282.
[13] W.Z. Chen, J.L. Hao, Z.Y. Chen, A study of self-burial of a radioactive waste container by deep rock melting, Sci. Technol. Nucl. Install (2013), https://doi.org/10.1155/2013/184757.
[14] P.A. Litsek, A. Bejan, Sliding contact melting: the effect of heat transfer in the solid parts, J. Heat Tran. 112 (1990) 808–812.

[15] A.J. Fowler, A. Bejan, Contact melting during sliding on ice, Int. J. Heat Mass Tran. 36 (5) (1993) 1171–1179.
[16] J.V.C. Vargas, A. Bejan, A. Dobrovicescu, The melting of an ice shell on a heated horizontal cylinder, J. Heat Tran. 116 (1994) 702–708.
[17] M. Oka, V.P. Carey, A unified treatment of the direct contact melting processes in several geometric cases, Int. Commun. Heat Mass Tran. 23 (2) (1996) 187–202.
[18] W.Z. Chen, S.M. Cheng, Z. Lou, An analytical solution of melting around a moving elliptical heat source, J. Therm. Sci. 3 (1) (1994) 23–27.
[19] M. Gong, W.Z. Chen, Y.S. Zhao, B. Zhu, F.R. Sun, Analysis of contact melting around a horizontal elliptical cylinder heat source, Prog. Nat. Sci. 18 (6) (2008) 441–446.
[20] M.A. Pudovcin, A.N. Salamatin, S.A. Fomin, V.K. Chistyakov, Effect of the working surface shape of a thermal drill on hot-point ice boring performance, J. Soviet Math. 43 (3) (1988) 2496–2505.
[21] S.A. Fomin, S.M. Cheng, Optimization of the heating surface shape in the contact melting problem, in: Third International Conference on Inverse Design Concepts and Optimization in Engineering Sciences, 1991, pp. 136–143. Washington D.C, Jan.
[22] M. Judd, An Introduction to the Engineering of Fast Nuclear Reactors, Cambridge University Press, New York, 2014.
[23] W.Z. Chen, Y.S. Zhao, F.R. Sun, Z.Y. Chen, M. Gong, Analysis of △T-driven contact melting of phase change material around a horizontal cylinder, Energy Convers. Manag. 49 (5) (2008) 1002–1007.
[24] A.N. Salamatin, S.A. Fomin, V.K. Chistyakov, V.A. Chugunov, Mathematical description and calculation of contact melting, J. Eng. Phys. 47 (1984) 1071–1077.
[25] A. Bejan, Contact melting heat transfer and lubrication, Adv. Heat Tran. 24 (1994) 1–38.
[26] X.C. Cui, Y.J. Jin, Z. Zhang, C. Liu, Numerical Simulation of inner-outer cooling flow field and temperature field for slab continuous casting, J. Iron Steel Res. 8 (2007) 14–18 (in Chinese) 19.
[27] M.K. Moallemi, R. Viskanta, Experimental on fluid flow induced by melting around a migrating heat source, J. Fluid Mech. 157 (1985) 35–51.
[28] J. Song, Q.A. Xiang, J. Deng, H.X. Yu, J. Du, J.S. Bi, Research on debris in-core cooling and retention characteristics, Nucl. Power Eng. 5 (2020) 193–196 (in Chinese) 40.